

Electronic Supporting Information

Ring-opening copolymerization of ϵ -caprolactone and δ -valerolactone by Titanium-based metal-organic framework

Rahaman M. Abdur,^{abc} Bibimaryam Mousavi,^{*a} Hossain M. Shahadat,^{abd} Nishat Akther,^e Zhixiong Luo,^a Serge Zhuiykov,^f and Francis Verpoort^{*af}

^a Laboratory of Organometallics, Catalysis and Ordered Materials, State Key Laboratory of Advanced Technology for Materials Synthesis and Processing, Wuhan University of Technology, Wuhan 430070, China.

^b School of Materials Science and Engineering, Wuhan University of Technology, Wuhan 430070, China.

^c Department of Chemistry, Mawlana Bhashani Science and Technology University, Santosh, Tangail-1902, Bangladesh.

^d Department of Chemistry, Comilla University, Cumilla 3506, Bangladesh

^e Department of Biochemistry and Molecular Biology, Mawlana Bhashani Science and Technology University, Santosh, Tangail-1902, Bangladesh

^f Center for Environmental and Energy Research, Ghent University, Global Campus, 119 Songdomunhwa-Ro, Yeonsu-Gu, Incheon 404-806, South Korea

Corresponding Authors: Francis Verpoort (Francis.verpoort@ghent.ac.kr),
Bibimaryam Mousavi (chem_moosavi2006@yahoo.com)

Contents

1. Experimental section	3
1.1. Materials	3
1.2. Synthesis of MIL-125	3
2. Characterization of catalyst MIL-125	4-6
FIGURE S1 PXRD of MIL-125	4
FIGURE S2 SEM images of MIL-125	4
FIGURE S3 FT-IR spectrum of MIL-125	5
FIGURE S4 TGA curve of MIL-125 ranging from 30 °C to 800 °C	5
FIGURE S5 The nitrogen adsorption-desorption isotherms for MIL-125	6
FIGURE S6 (a) NH ₃ -TPD and (b) CO ₂ -TPD profiles of MIL-125	6
3. Synthesis and characterizations of polymers	7-14
3.1. Synthesis of polymers	7
3.2. Characterizations of polymers	7
FIGURE S7 Comparison of FT-IR spectra of PCL, PVL and poly(CL- <i>co</i> -VL)	8
FIGURE S8 ¹ H NMR spectra of copolymers obtained at different time	8
FIGURE S9 ¹³ C NMR of PCL and PVL	9
Randomness Calculation	9
Reactivity ratio	9
TABLE S1 Molar feed ratio of the monomers and copolymer composition	10
FIGURE S10 Reactivity ratio analysis of CL and VL	10
FIGURE S11 ¹ H- ¹³ C HMBC NMR spectrum of Poly(CL- <i>co</i> -VL)	11
FIGURE S12 GPC traces of obtained Poly(CL- <i>co</i> -VL)	11
TABLE S2 Kinetics study of the copolymerization	12
FIGURE S13 Dependence of <i>M_n</i> and <i>D</i> on monomer conversion	12
FIGURE S14 Kinetics study for Poly(CL- <i>co</i> -VL) synthesis	13
Table S3 Thermal behaviour of synthesized copolymers	13
FIGURE 15 MALDI-TOF MS spectra of low molecular weight poly(CL- <i>co</i> -VL) copolymer	13
TABLE S4 Assignment of calculated and experimental MALDI-TOF MS signals	14
TABLE S5 Copolymerization of CL with VL initiated with the components of MIL-125	14
4. Comparison between before and after polymerization	15-16
FIGURE S16 PXRD patterns of MIL-125 before and after the polymerization reaction	15
FIGURE S17 SEM images of MIL-125 before and after the polymerization reaction	15
TABLE S6 Metal content in MIL-125 before and after polymerization	16
TABLE S7 Catalyst (MIL-125) recycling studies	16
References	16

1. Experimental section

1.1. Materials. Benzene-1,4-dicarboxylic acid (BDC; 98%), titanium isopropoxide ($\text{Ti}(i\text{PrO})_4$; 97%), CL (purity ~99%) and VL (98%) were purchased from the commercial supplier (Aladdin Chemical Co. Ltd.). CL and VL were used after two times distillation over CaH_2 under reduced pressure. All reagents and solvents were analytical grade and used as received from the supplier without further purification.

1.2. Synthesis of MIL-125. MIL-125 was synthesized by the reflux method according to the known procedure with slight modification.¹ BDC (1.2 g, 7.2 mmol) was dissolved in dry DMF (40 mL) and stirred it in a three-necked round bottom flask with a reflux condenser under an inert atmosphere at 110 °C for 1 h. After that, anhydrous MeOH (approximately 10 mL) was added to the solution and heated again for 1 h at 110 °C under stirring and reflux conditions. However, $\text{Ti}(i\text{PrO})_4$ (1.5 mL, 5 mmol) was added into the solution dropwise and the resulting solution was refluxed at 110 °C for 72 h to crystallize. Thereafter the reaction mixture was cooled to room temperature, and the white crystalline product was isolated with the help of centrifugation. For further purification, the as-synthesized product was re-dispersed at 60 °C in fresh DMF (200 mL) for 2 h and then in MeOH for 2 h. After cooling, the product was washed with fresh MeOH three times and finally dried at 80 °C under vacuum overnight.

2. Characterization of catalyst MIL-125.

The crystallinity of the catalyst was investigated by powder X-ray diffraction (PXRD) analysis ($2\theta = 5\sim 60^\circ$) using PANalytical Empyrean instrument with monochromatic $\text{Cu-K}\alpha$ radiation ($\lambda = 1.54184 \text{ \AA}$) at a scan rate of $2^\circ/\text{min}$. The catalyst's morphology was determined with a scanning electron microscope (SEM) from JEOL (JSM-IT300, 0.5–35 kV). Fourier transform infrared spectroscopy (FTIR; Bruker Vertex 80V) was performed to confirm the presence of metal-linker coordination in the MIL-125 structure in the wave range of $4000\text{--}400 \text{ cm}^{-1}$. The stability of the catalyst was checked by thermogravimetric analysis (TGA) (Netzsch; STA 449C) at 25 to 800 °C ($5^\circ/\text{min}$ as the heating rate) under N_2 flow ($20 \text{ mL}/\text{min}$). The Brunauer-Emmett-Teller (BET) surface area and porosity were measured with the help of Micromeritics ASAP 2020 equipment following N_2 sorption isotherms, and thereby the sample (MIL-125) was activated at 150 °C for 4 h under vacuum before the measurement. Temperature programmed desorption (TPD) profile of NH_3 and CO_2 from the catalyst were determined using a Micromeritics chemisorb 2750 Pulse Chemisorption.

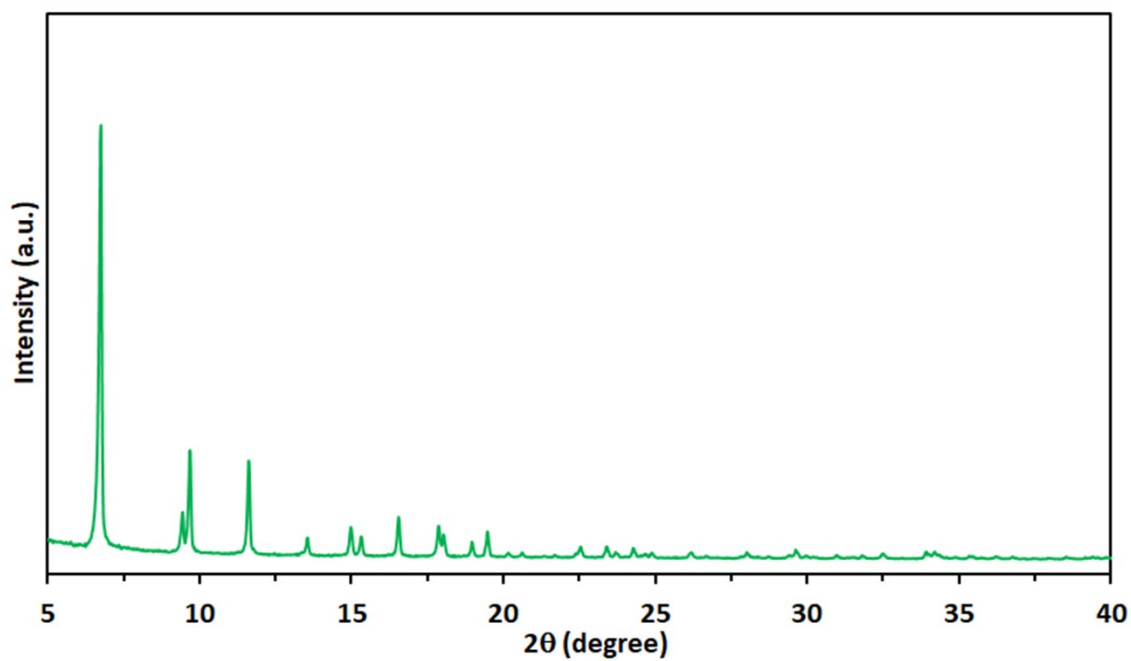


FIGURE S1 PXRD of MIL-125. All sharp diffraction peaks show the characteristics of MIL-125 and identical to the reported one.¹⁻²

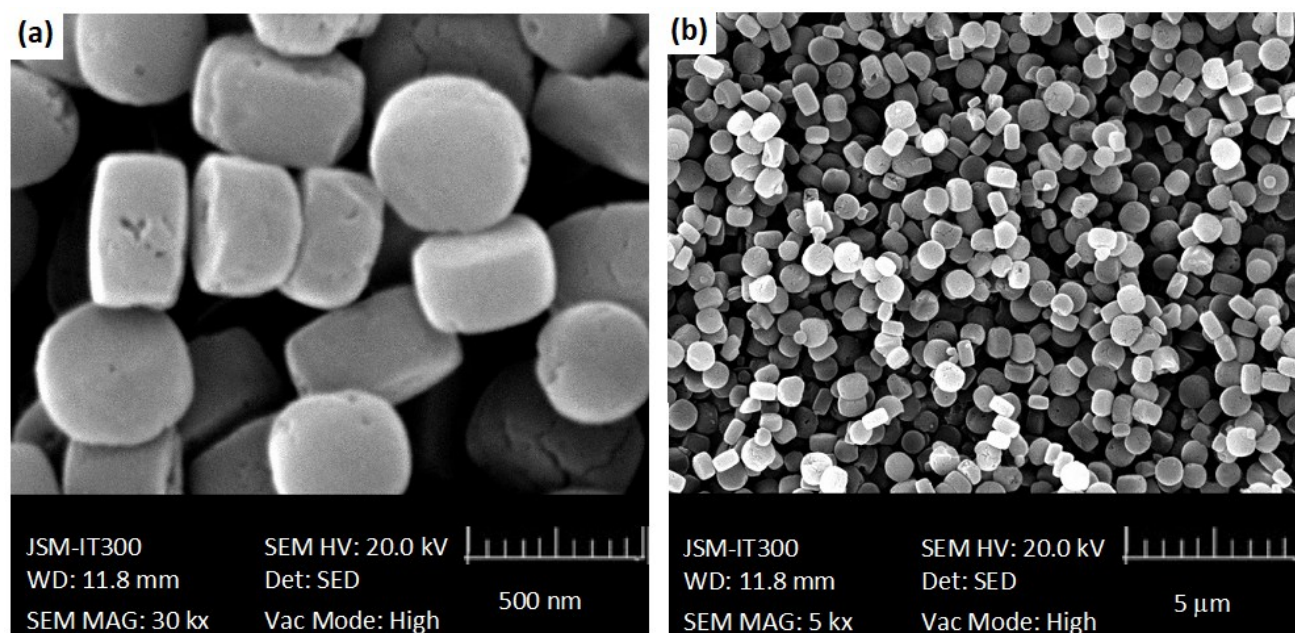


FIGURE S2 SEM images of MIL-125: (a) 500 nm and (b) 5 μm scale. Disk-like shape of MIL-125 is formed with the average particle size in the range of 0.3-0.5 μm .

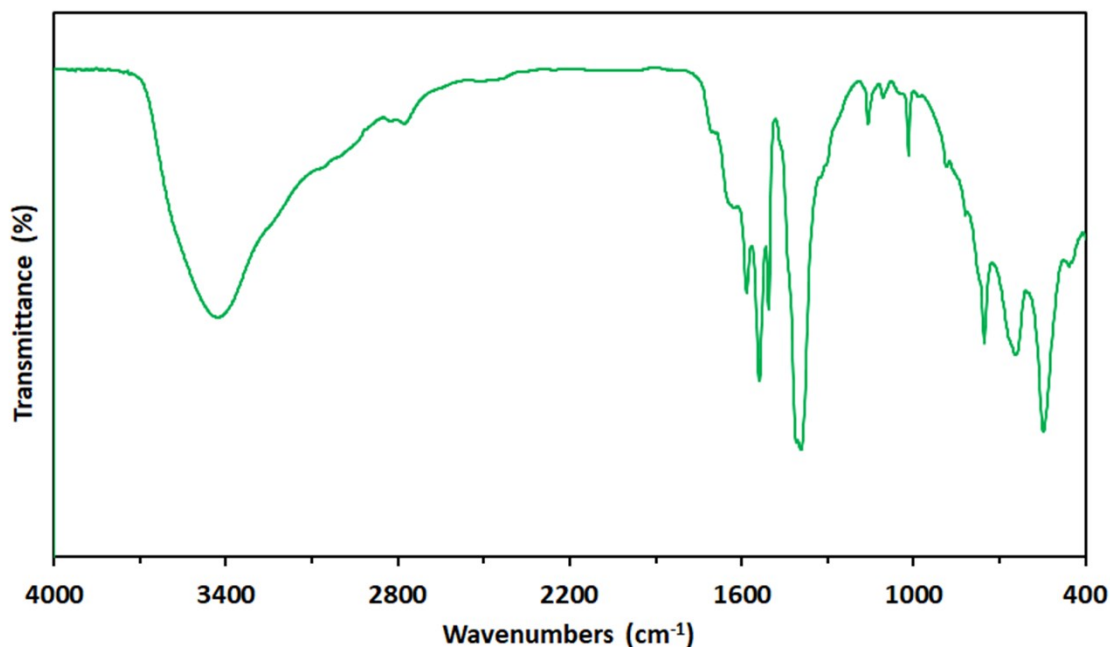


FIGURE S3 FT-IR spectrum of MIL-125. The characteristics absorption peaks at 800-400 cm⁻¹ reveal strong indication of O-Ti-O metal-organic nature.²⁻³ The absence of absorption peaks at 1710 cm⁻¹ designates the nonexistence of free H₂BDC linkers. And other absorption peaks in the FT-IR spectrum confirm the successful formation of MIL-125.⁴

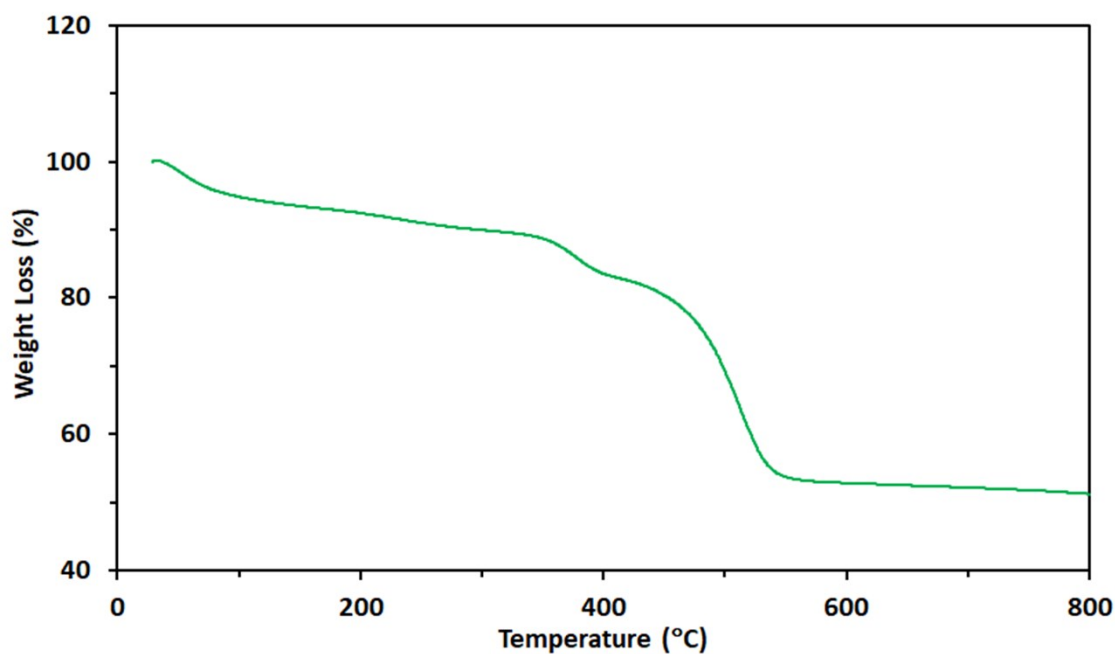


FIGURE S4 TGA curve of MIL-125 ranging from 30 °C to 800 °C. It shows the first weight loss of MIL-125 around 180 °C, which may be associated with the removal of remaining solvent molecules.

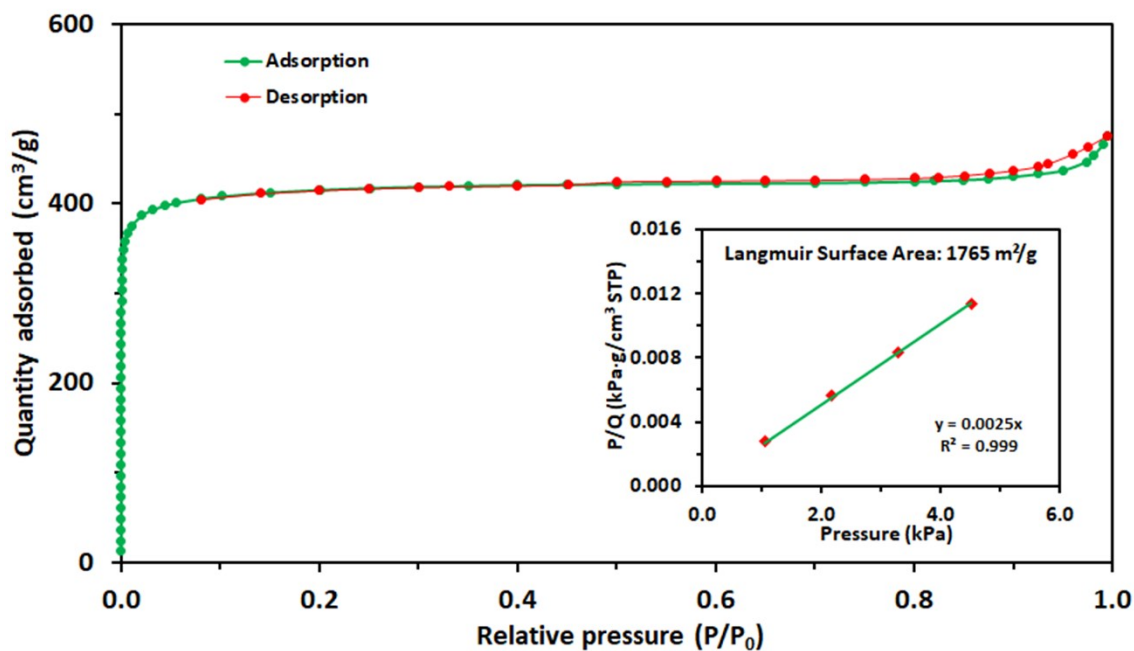


FIGURE S5 The nitrogen adsorption-desorption isotherms for MIL-125 measured at 77K. The specific surface area estimated by the Brunauer–Emmett–Teller (BET) method and the total pore volume are $1670 \text{ m}^2 \text{ g}^{-1}$ and $0.73 \text{ cm}^3 \text{ g}^{-1}$, respectively, indicating a high surface area of MIL-125.

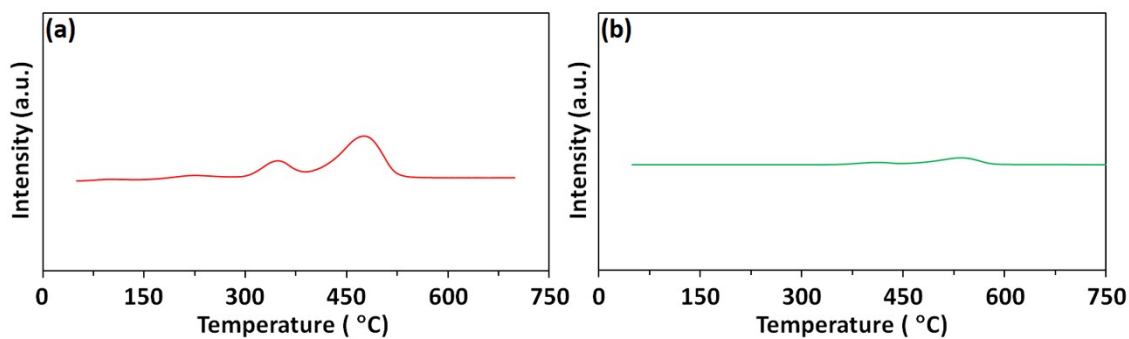


FIGURE S6 (a) NH_3 -TPD and (b) CO_2 -TPD profiles of MIL-125, whereas acid sites are more pronounced than its basic sites.

3. Synthesis and characterizations of polymers

3.1. Synthesis of polymers. Copolymers, poly(CL-co-VL) were synthesized in bulk by ROP, and all polymerization reactions performed in a standard Schleck flask under an inert atmosphere. Prior to use, the catalyst was activated at 150 °C under vacuum for 12 h. As for the typical polymerization procedure, a predetermined amount of activated MIL-125 (0.025 mmol), CL (1.25 mmol), and VL (1.25 mmol) ([CL]/[VL]/[MIL-125]=50/50/1) were loaded in a standard Schleck flask successively inside the glovebox at room temperature. Then the flask was sealed carefully and placed in a pre-heated oil bath at a constant temperature. After a certain time, the polymerization reactions were terminated by cooling the flask in an ice bath. After cooling and quenching the mixture, the monomer conversion was calculated by ¹H-NMR detection using solvent CDCl₃. The crude mixture was then dissolved in minimum amount of CHCl₃ and filtered to separate the MIL-125 catalyst and put the filtrate in the open air for evaporation until to dry completely. Later on, the copolymer was precipitated by adding a large excess of cold methanol. After washing with fresh methanol, the polymer product was dried at 50 °C under vacuum for 24 h. Besides, the copolymers with different ratios and low conversion (<10%) were prepared for calculating the reactivity ratio.

3.2. Characterizations of polymers. ¹H- and ¹³C-NMR spectra of the synthesized polymers were recorded on a Bruker AC-500 NMR spectrometer using CDCl₃ as the solvent and tetramethylsilane (TMS) as an internal standard. FTIR spectroscopy was performed with a Bruker Vertex 80 V FTIR spectrometer. The differential scanning calorimetry (DSC) analysis was conducted using NETZSCH STA 449C instruments. The samples were scanned from RT to 100 °C at a heating rate of 10 °C/min to remove the moisture and then cooled to -70 °C at 5 °C/min (cooling scan rate). And finally, it was scanned again from -70 °C to 120 °C at a heating rate of 5 °C/min (heating scan). The glass transition temperature (T_g) and melting temperature (T_m) were measured from cooling and heating scan graphs, respectively. Molecular weight (M_n) and the dispersity (\mathcal{D}) of the polymers were determined by PL-GPC 50 with PLgel 5 μ m MIXED-C column (300mm \times 7.5mm), Agilent Technology in THF (Fisher, HPLC grade, stabilized with BHT, 2.5ppm) using polystyrene (PS) as a standard. Before determining molecular weights, samples were dissolved in THF (Fisher, HPLC grade, stabilized with BHT, 2.5 ppm) for 24 h and then filtered where the concentration was maintained around 2.5 mg mL⁻¹. Matrix-assisted laser desorption ionization-time of flight mass spectroscopy (MALDI-TOF MS) of low molecular weight polymeric sample was performed using Bruker ultrafleXtremeTM spectrometer. Here, α -cyano- 4-hydroxycinnamic acid was used as a matrix. Moreover, induced coupled plasma (ICP) was performed for both solution mixture and resultant copolymers under Ar gas flow (0.3MPa).

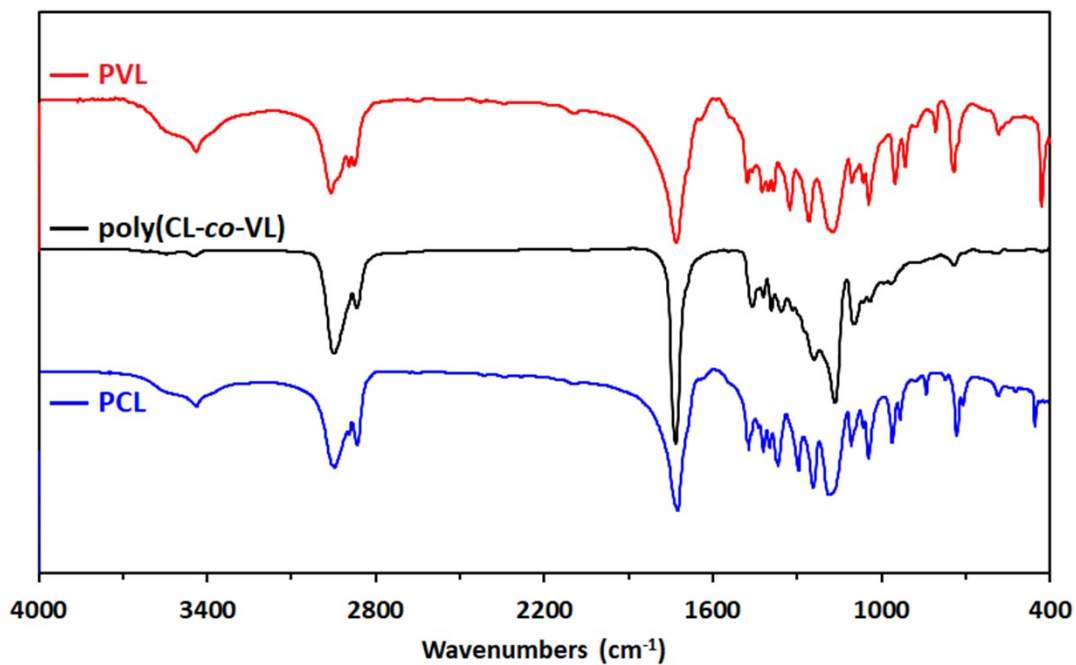


FIGURE S7 Comparison of FT-IR spectra of PCL, PVL and poly(CL-co-VL).

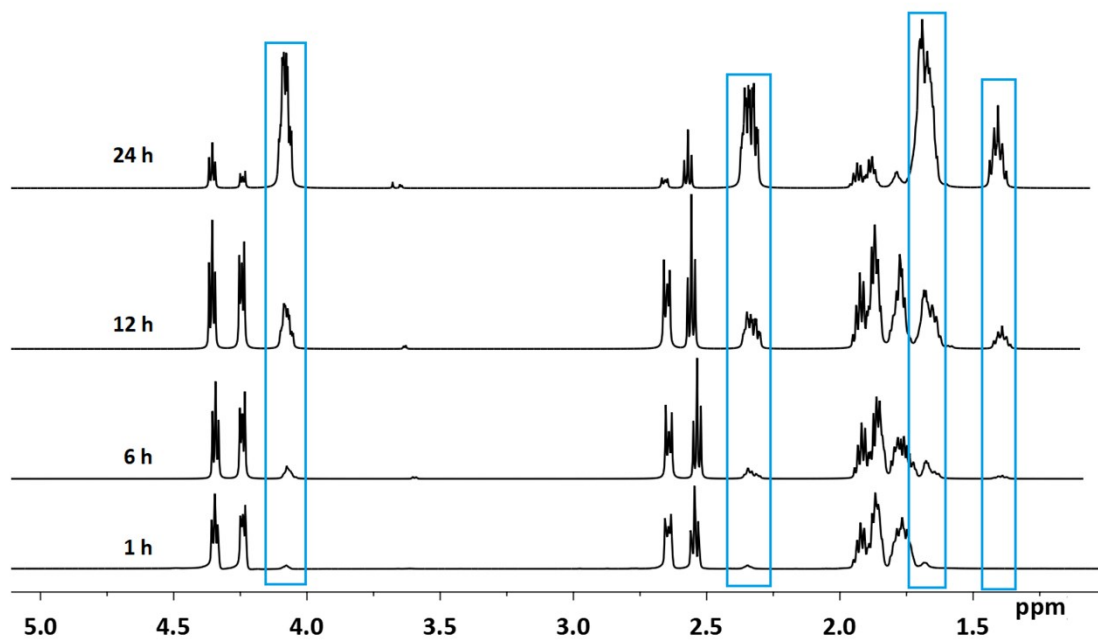


FIGURE S8 ^1H NMR spectra of copolymers obtained at different time.

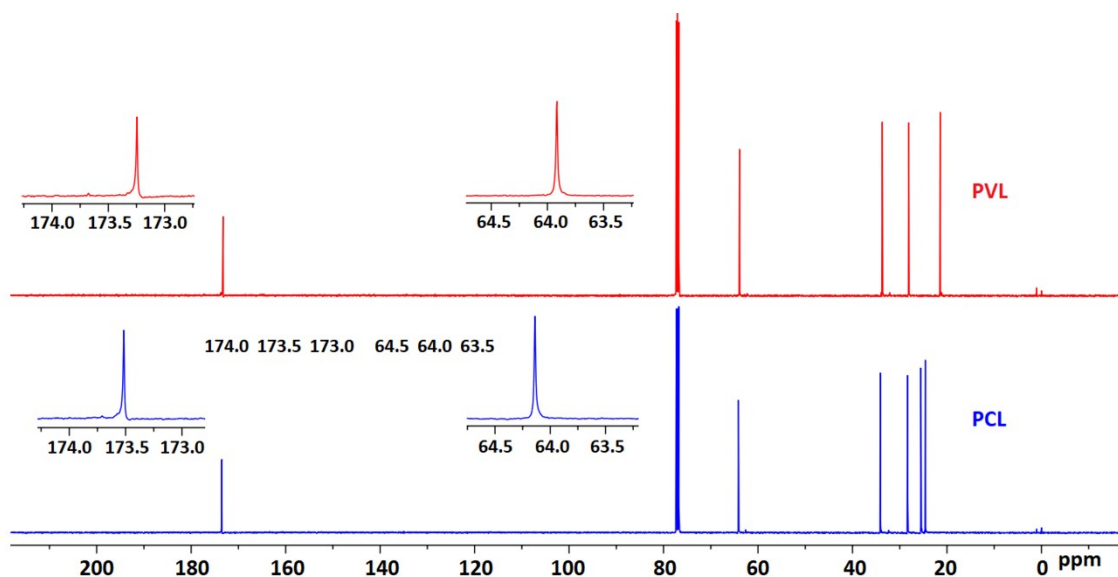


FIGURE S9 ^{13}C NMR of PCL (Table 1, entry 1) and PVL (Table 1, entry 7).

Randomness Calculation

By following given equations, the average sequence length (L) and degree of randomness (R) were calculated which are related to the peak area in ^{13}C NMR.⁵

$$\begin{aligned}
 &\text{Sequence length of CL unit in copolymer, } L_c = \frac{l_{cc}}{l_{vc}} + 1 & R = \frac{1}{L_c} + \frac{1}{L_v} \\
 &\text{Sequence length of VL unit in copolymer, } L_v = \frac{l_{vv}}{l_{cv}} + 1 & R=0; \text{ block copolymer} \\
 & & R=1; \text{ random copolymer} \\
 & & R=2; \text{ alternating copolymer}
 \end{aligned}$$

Where, l_{cc} , l_{vc} , l_{vv} and l_{cv} represents the integral area of peaks at 64.14, 63.83, 63.91 and 64.21 ppm region in ^{13}C NMR of poly(CL-co-VL) (Fig. 3). Here, R values are found equal to 1 in the whole range of composition which confirm the formation of random copolymer.

Reactivity ratio

Using the method of Fineman-Ross, the reactivity ratio of CL and VL was calculated.⁶ At low monomer conversion various copolymers were prepared and their compositions were calculated by ^1H NMR.

$$\frac{F(f-1)}{f} = r_1 \frac{F^2}{f} - r_2$$

Thus, a plot of $\frac{F(f-1)}{f}$ vs. $\frac{F^2}{f}$ yields a straight line with slope equal to r_1 and intercept to r_2 .

TABLE S1 Molar feed ratio of the monomer CL and VL, and copolymer composition of Poly(CL-co-VL).

CL:VL	F ^a	f ^b	F ² /f	F(f-1)/f	r ₁	r ₂	r ₁ r ₂
85:15	5.67	6.14	5.23	4.74			
65:35	1.86	1.56	2.21	0.67			
50:50	1.00	1.04	0.96	0.04	1.0488	0.9921	1.0405
35:65	0.54	0.59	0.49	-0.38			
15:85	0.18	0.23	0.13	-0.58			

^a molar ratio of CL to VL in reaction mixture; ^b molar ratio of CL to VL in copolymer determined by ¹H NMR spectroscopy; r₁ and r₂, the reactivity ratio of CL and VL, respectively.

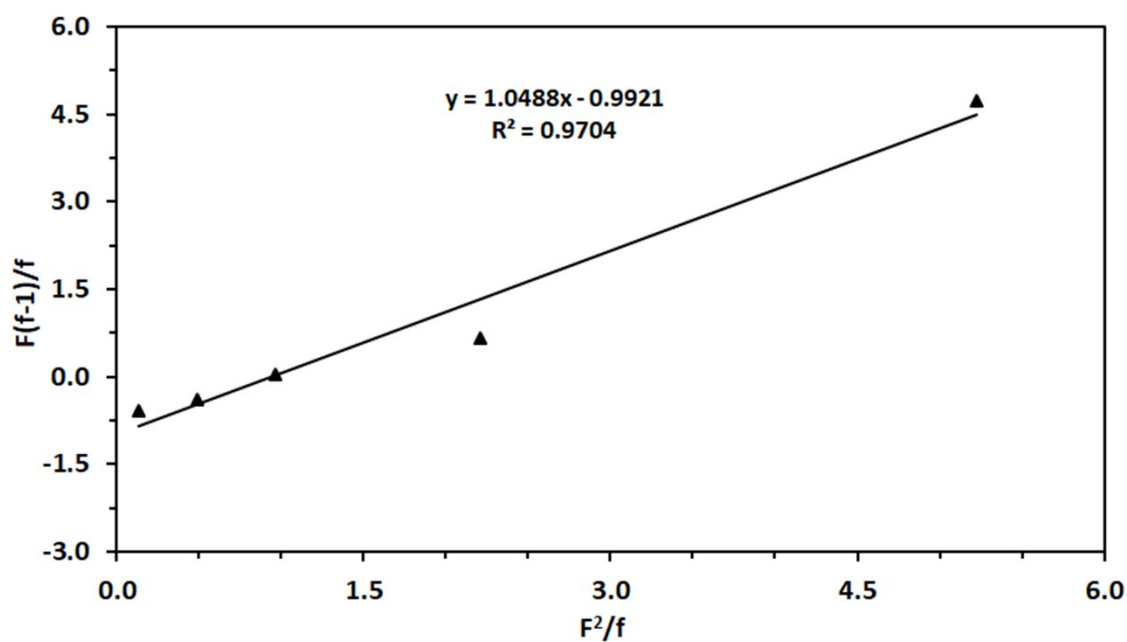


FIGURE S10 Reactivity ratio analysis of CL and VL.

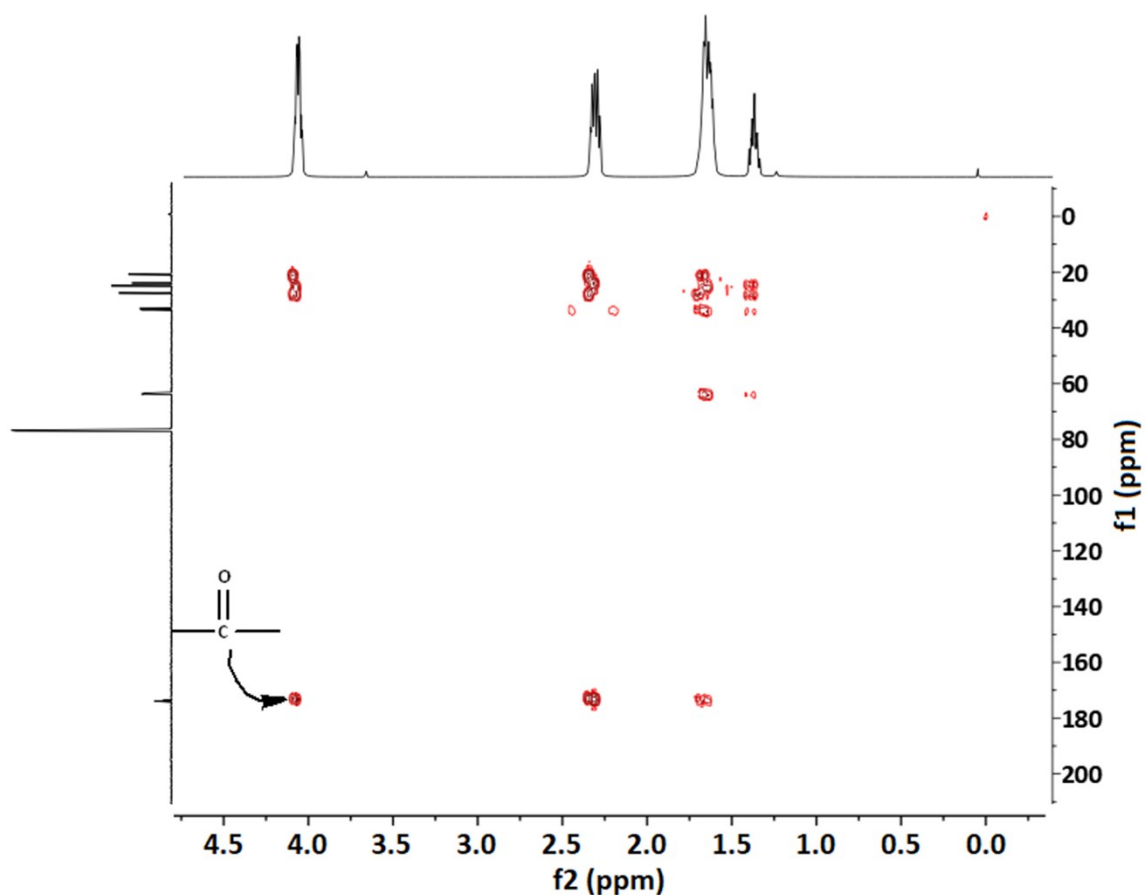


FIGURE S11 ^1H - ^{13}C HMBC NMR spectrum of Poly(CL-co-VL) initiated by MIL-125 (Table 1, entry 4).

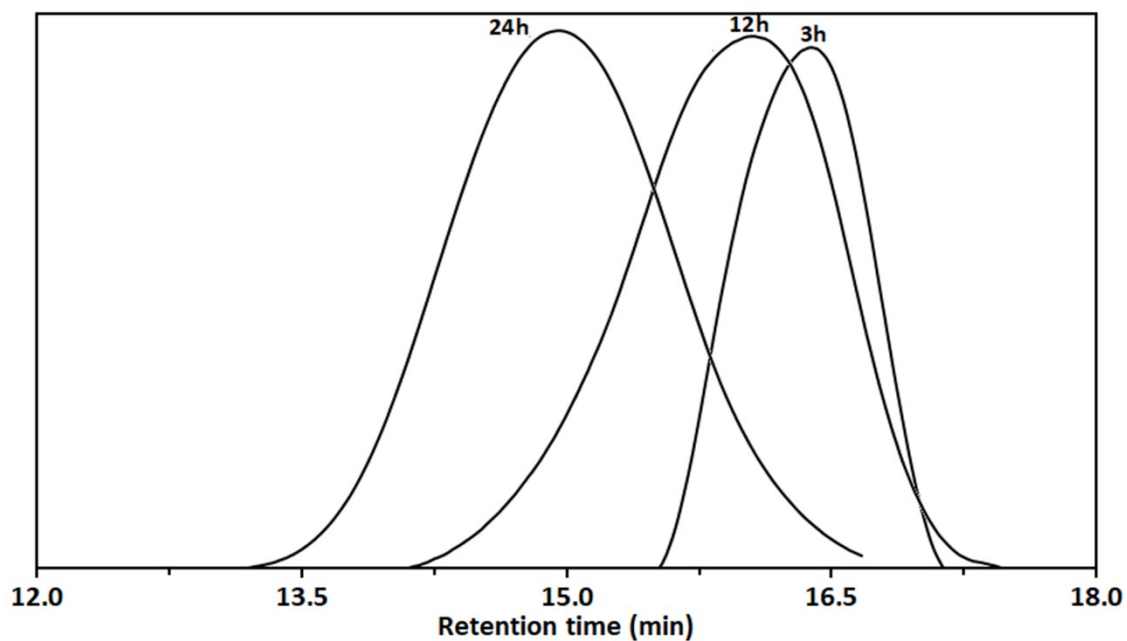


FIGURE S12 GPC traces of obtained Poly(CL-co-VL) at different time with 50/50 molar feed ratio of CL/VL (eluent THF, flow rate 1.0 mL/min, PS standard).

TABLE S2 Kinetics study of the copolymerization of CL with VL using MIL-125 in bulk at 140 °C^a.

entry	time (h)	conv. ^b (%)		M_n ^c (kg/mol)	\bar{D} ^c
		CL	VL		
1	0	0	0	-	-
2	1	7	7	2.0	1.11
3	3	10	10	4.9	1.15
4	6	29	27	5.2	1.16
5	9	46	45	9.1	1.34
6	12	72	70	12.2	1.54
7	24	95	89	20.2	1.64

^a molar feed ratio of CL and VL=50; ^b conversion determined by ¹H NMR spectroscopy in CDCl₃; ^c number average molecular weight and dispersity measured by GPC with polystyrene calibration.

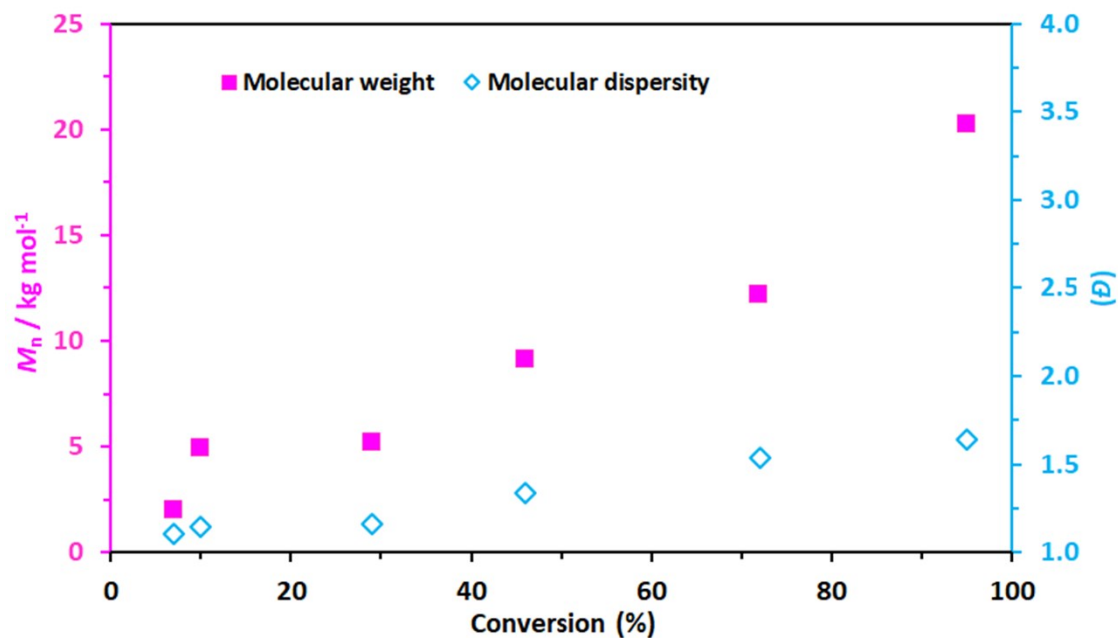


FIGURE S13 Dependence of molecular weight (M_n) and dispersity (\bar{D}) on monomer conversion for poly(CL-co-VL) synthesis using MIL-125.

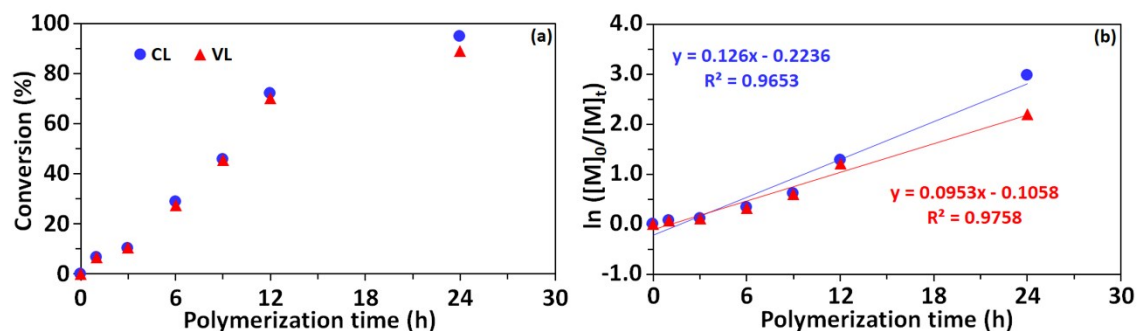


FIGURE S14 Kinetics study for Poly(CL-co-VL) synthesis: (a) conversion of monomer CL and VL with polymerization time (b) $\ln([M]_0/[M]_t)$ vs. polymerization time of each monomer at molar feed ratio of CL and VL = 50:50 and 140 °C.

Table S3 Thermal behaviour of synthesized copolymers

entry	(CL:VL) ^a	T_m (°C)	T_g (°C)	ΔH_m (Jg ⁻¹)	R^b
1	100:0	59.4	-56.2	77.21	-
2	85:15	23.8	-66.5	72.53	1.00
3	65:35	22.4	-61.7	67.95	1.00
4	50:50	21.2	-66.7	66.50	1.00
5	35:65	22.0	-61.5	64.26	1.00
6	15:85	25.1	-66.4	56.54	1.00
7	0:100	62.1	-55.7	87.85	-

^a molar feed ratio of CL and VL; ^b degree of randomness, calculated from ¹³C NMR spectroscopy.

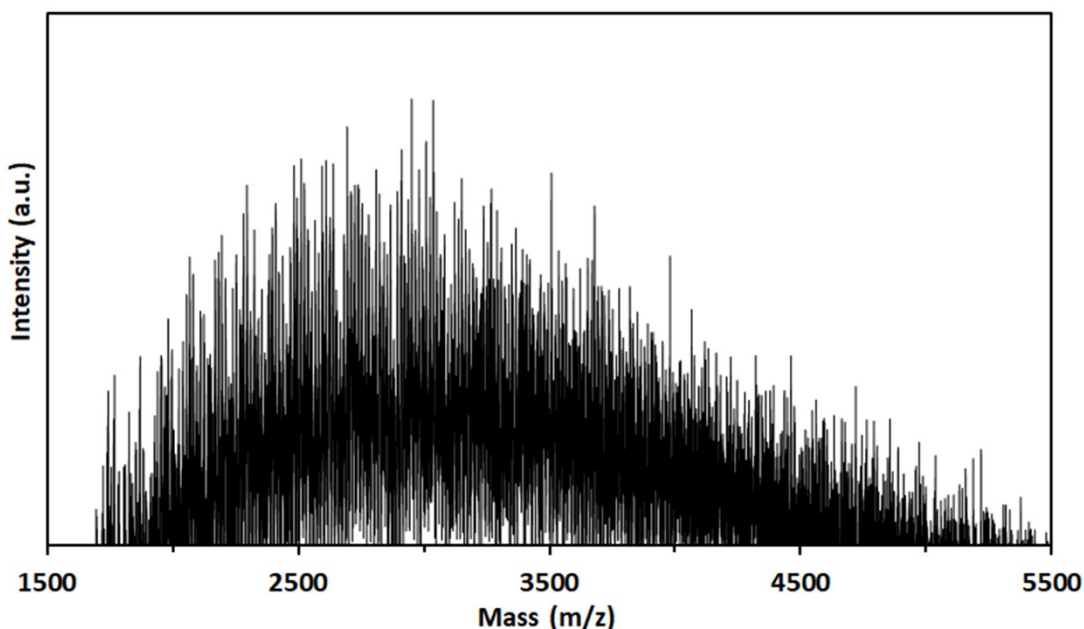


FIGURE S15 MALDI-TOF MS spectra of low molecular weight poly(CL-co-VL) copolymer.

TABLE S4 Assignment of calculated and experimental MALDI-TOF MS signals.

N^a	m^b	n^b	m/z (cal.)	m/z (exp.)	Structure ^c
24	11	13	2580.10	2580.73	Cyclic
	12	12	2594.12	2594.67	Cyclic
25	11	14	2680.22	2680.85	Cyclic
	13	12	2708.26	2708.50	Cyclic
26	11	15	2780.34	2779.78	Cyclic
	14	12	2822.40	2822.64	Cyclic
27	11	16	2880.46	2879.85	Cyclic
	15	12	2936.54	2937.13	Cyclic
28	11	17	2980.58	2980.33	Cyclic
24	11	13	2598.12	2598.12	Linear
	12	12	2612.14	2610.54	Linear
25	11	14	2698.24	2697.62	Linear
	13	12	2726.28	2727.60	Linear
26	11	15	2798.36	2798.49	Linear
	14	12	2840.42	2840.99	Linear
27	11	16	2898.48	2898.55	Linear
	15	12	2954.56	2953.17	Linear
28	11	17	2998.60	2998.01	Linear

^atotal number of repeating units in copolymer; ^b number of CL or VL repeating units; ^c for cyclic follows $114.12m + 100.12n + 23$ and for linear follows $114.14m + 100.12n + 18.015 + 23$ formula.

TABLE S5 Copolymerization of CL with VL initiated with the components of MIL-125^a

entry	catalyst	conv.^b (%)		M_n^c (kg/mol)	Đ^c
		CL	VL		
1	benzene-1,4-dicarboxylic acid [BDC]	29	40	30.5	1.50
2	titanium isopropoxide [Ti(<i>i</i> PrO) ₄]	99	96	50.1	1.21

^a molar feed ratio of CL and VL = 50:50, temperature = 140 °C and time = 24 h; ^b conversion determined by ¹H NMR spectroscopy in CDCl₃; ^c number average molecular weight and dispersity measured by GPC with polystyrene calibration.

4. Comparison between before and after polymerization

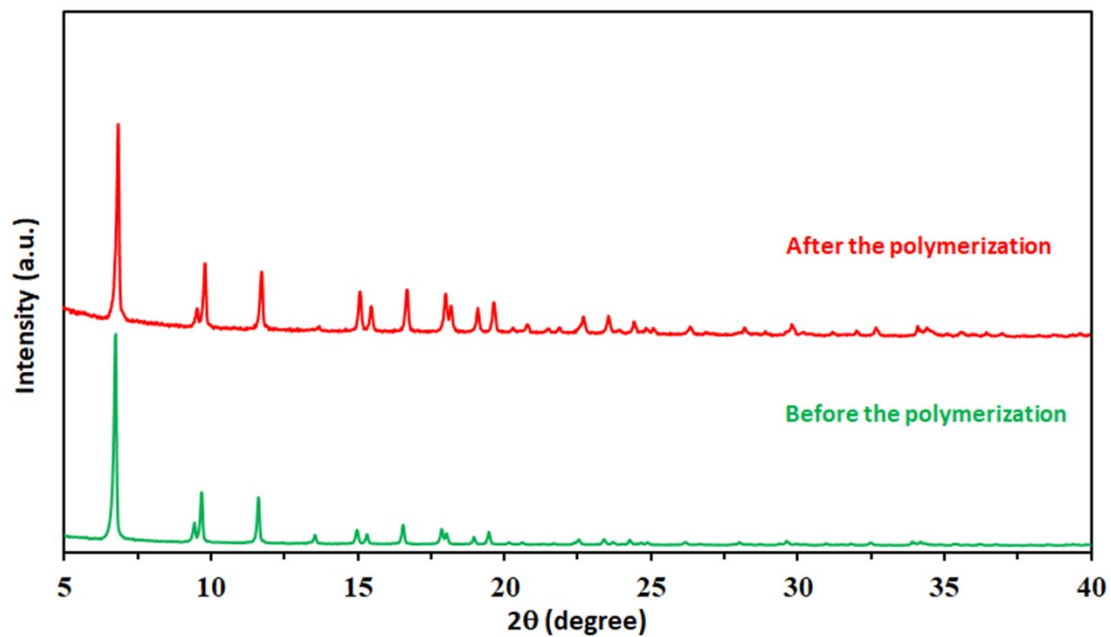


FIGURE S16 PXRD patterns of MIL-125: before (bottom) and after (top) the polymerization reaction.

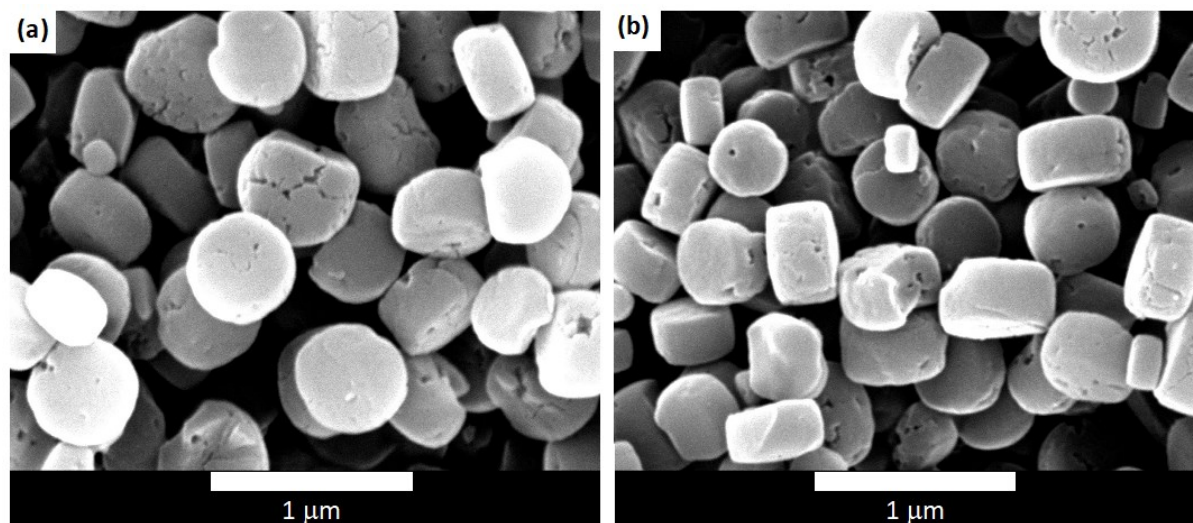


FIGURE S17 SEM images of MIL-125: before (a) and after (b) the polymerization reaction.

TABLE S6 Metal content in MIL-125 before and after polymerization reaction along with poly(CL-co-VL) by ICP analysis.

entry	sample	Ti (wt.%)
1	Pristine MIL-125	25.09
2	Recovered MIL-125 (3 rd cycle)	24.48
3	Poly(CL-co-VL) ^a	No

^a molar feed ratio of CL and VL = 50:50; temperature = 140 °C; time = 24 h.

TABLE S7 Catalyst (MIL-125) recycling studies.

run ^a	conv. ^b (%)		M_n ^c (kg/mol)	\bar{D} ^c
	CL	VL		
1	95	89	20.2	1.64
2	94	89	19.9	1.61
3	93	88	18.4	1.56

^a molar feed ratio of CL and VL = 50:50, temperature = 140 °C and time = 24 h; ^b Calculated by ¹H-NMR using CDCl₃; ^cDetermined by GPC analysis in THF at room temperature referenced to polystyrene standards.

References

- 1 I. D. Ivanchikova, J. S. Lee, N. V. Maksimchuk, A. N. Shmakov, Y. A. Chesalov, A. B. Ayupov, Y. K. Hwang, C. H. Jun, J. S. Chang and O. A. Kholdeeva, *Eur. J. Inorg. Chem.*, 2014, **2014**, 132.
- 2 W. P. Mounfield, C. Han, S. H. Pang, U. Tumuluri, Y. Jiao, S. Bhattacharyya, M. R. Dutzer, S. Nair, Z. Wu, R. P. Lively, D. S. Sholl and K. S. Walton, *J. Phys. Chem. C*, 2016, **120**, 27230.
- 3 J. G. Santaclara, M. A. Nasalevich, S. Castellanos, W. H. Evers, F. C. M. Spoor, K. Rock, L. D. A. Siebbeles, F. Kapteijn, F. Grozema, A. Houtepen, J. Gascon, J. Hunger and M. A. van der Veen, *ChemSusChem*, 2016, **9**, 388.
- 4 M. Dan-Hardi, C. Serre, T. Frot, L. Rozes, G. Maurin, C. Sanchez and G. Férey, *J. Am. Chem. Soc.*, 2009, **131**, 10857.
- 5(a) T. Wu, Z. Wei, Y. Ren, Y. Yu, X. Leng and Y. Li, *Polym. Degrad. Stabil.*, 2018, **155**, 173; (b) M. T. Hunley, N. Sari and K. L. Beers, *ACS Macro Letters*, 2013, **2**, 375; (c) N. Nomura, A. Akita, R. Ishii and M. Mizuno, *J. Am. Chem. Soc.*, 2010, **132**, 1750.
- 6(a) M. Fineman and S. D. Ross, *J. Polym. Sci.*, 1950, **5**, 259; (b) W. Ritchey and L. Ball, *J. Polym. Sci. Pol. Lett.*, 1966, **4**, 557; (c) B. S. Beckingham, G. E. Sanoja and N. A. Lynd, *Macromolecules*, 2015, **48**, 6922.